ESIA15 & ISSI-2019 Joint Conference on
Engineering Structural Integrity Assessment

CREEP-FATIGUE LIFE ASSESSMENT OF HYDROGENATION REACTOR MANUFACTURED OF 2.25CR-1MO STEEL USING THE LINEAR MATCHING METHOD FRAMEWORK

Zhiyuan Ma[a], Xiaoxiao Wang[a], Haofeng Chen[a,b*], Fuzhen Xuan[b]

Keywords: Creep, Low-cycle fatigue, Hydrogenation reactor, 2.25Cr-1Mo steel, Finite element analysis.

This paper presents a creep-fatigue life assessment of a typical hydrogenation reactor made of 2.25Cr-1Mo steel and subjected to inner pressure and thermal gradient using the Linear Matching Method (LMM) framework. The LMM framework has been implemented as a plug-in with a graphic user interface within the commercial finite element software ABAQUS for improved usability and accuracy. The study is performed with the latest developed extended Direct Steady Cycle Analysis (eDSCA) module for creep-fatigue interaction assessment. The design operating condition is determined by the shakedown analysis using corresponding modules in the LMM framework. The creep-fatigue analysis is then conducted using the Ramberg-Osgood (R-O) model considering temperature-dependent stress-strain relationship for cyclic steady-state plastic behaviour and non-isothermal Norton-Bailey model for creep strain evaluation. Damage assessment considers time fraction rule for creep damage evaluation, ε-N curve and total strain range for fatigue damage evaluation, and bi-linear damage rule for total creep-fatigue damage evaluation. The influence of dwell time and internal pressure on the number of cycles to failure has been studied. Based on that, a series of analytic functions have been formulated for practical use in the petrochemical industry.

INTRODUCTION

In the field of petrochemical engineering, typical industrial processes such as hydrodesulphurization and hydrocracking are often conducted using various types of hydrogenation reactors. Operating in the hydrogen environment with high temperature and high pressure, the hydrogenation reactor has become one of the most critical pressure vessels that require systematic creep-fatigue assessment. The reason is that the damage caused by creep-fatigue interaction is considered as a critical factor which restricts the life span of hydro-processing equipment (Wu et al. [1]). On the level of structural creep-fatigue analysis, a phenomenon called creep ratchetting can often be observed while cyclic plasticity and creep interacting with each other. Some important phenomena called “cyclically enhanced creep” and “creep enhanced plasticity” may

a. Department of Mechanical & Aerospace Engineering, University of Strathclyde, James Weir Building, 75 Montrose Street, Glasgow G1 1XJ, UK; b. School of Mechanical and Power Engineering, East China University of Science and Technology, 200237, China. Corresponding author: haofeng.chen@strath.ac.uk

also be observed, (Barbera [2]) which are mainly caused by large stress relaxation and non-closed hysteresis loop for structures in non-isothermal operating conditions. For pure fatigue damage evaluation, there exist several methodologies and international design codes including the Neuber's rule based on linear elastic analysis (Zheng et al. [3]) and the elastic-plastic method considered in ASME VIII-2 [4], similarly for pure creep damage evaluation. However, few design procedures have provided complete creep-fatigue interaction damage assessment. Released in 2008 and updated in 2015, the Code Case 2605 [5] of ASME BPV VIII-2 offers a series of creep-fatigue life prediction curves for hydrogenation reactors operating at temperatures higher than 371 ºC and less than 500 ºC. CC 2605 includes Omega creep constitutive equations and creep-affected fatigue design curves, and introduces a complete appraisal procedure containing shakedown analysis, pure creep damage evaluation and creep-fatigue interaction assessment. It also requires a cycle-by-cycle inelastic analysis if the simplification criteria are not satisfied. However, it is widely acknowledged that complete inelastic analysis is highly time-consuming and cost-inefficient. Thus, direct methods have been proposed to assess structural behaviours quickly and efficiently by making a few reasonable assumptions. Recently a novel direct method, the extended Direct Steady Cycle Analysis (eDSCA) within the Linear Matching Method (LMM) framework (Barbera et al. [6]) has been proposed and proven to be a highly robust and efficient structural integrity solution. The LMM framework also consists of some other modules, such as shakedown limit evaluation using the Linear Matching Method (LMM) algorithm, ratchet limit evaluation, and low-cycle fatigue assessment using the Direct Steady Cycle Analysis (DSCA) algorithm. Therefore, the LMM procedure is capable of substituting some inelastic cycle-by-cycle analysis in design codes and solving industrial problems.

FINITE ELEMENT MODEL AND MATERIAL PROPERTIES

A typical hydrogenation reactor made of 2.25Cr-1Mo steel is modelled using the commercial finite element software ABAQUS to illustrate the investigation of creep-fatigue interaction, as shown in Fig. 1. The reactor is comprised of an inlet nozzle, a connection head, a cylindrical shell and an attachment flange. The inner diameter of the cylindrical tank is 1700mm, and the inner diameter of the inlet nozzle is 860mm. The thickness of the whole model varies from 38mm to 48mm, and the total axial length is 1950mm. It has been verified that the flange bores have little influence on the creep-fatigue assessment results, so an axisymmetric 2-D model is built for the sake of simplicity. The axial displacement is constrained at the bottom surface and the symmetry boundary condition is imposed around its rotation axis. A uniform pressure is applied on the internal surfaces of the reactor, and a corresponding pressure is applied at the top surface in the axial direction to simulate closed end boundary condition. Besides, a steady-state thermal analysis is performed to simulate the normal operating thermal condition. The model is meshed into 755 quadratic DCAX8 elements. Because of geometric discontinuities, the mesh is denser at the transition part between nozzle and reactor head.

The loading history for a typical hydrogenation operation cycle is shown in Fig. 2. The high-temperature mixture of oil and hydrogen is first pumped into the reactor which increases the temperature of the inner surface to around 450 ºC and causes a temperature gradient as shown in Fig. 1. Then the inner pressure rises to 10 MPa for hydrogenation reaction with the assistance of solid catalyst. After 9000 hours of dwell time, the pressure is released at the bottom end of the reactor and the temperature drops to the idle state. The high pressure is only engaged when the temperature reaches normal operation state to help prevent temper embrittlement failure of 2.25Cr-1Mo. With the presence of cyclic pressure, thermal stress and high-temperature creep dwell, structural responses of both fatigue and creep should be considered with care when conducting the life assessment of the hydrogenation reactor.

In terms of material properties, the cyclic plasticity constitutive equations are expressed in forms of Ramberg-Osgood (R-O) model to consider saturated cyclic stress-strain behaviour along with the Elastic-Perfectly-Plastic (EPP) model, as shown in Fig. 3a. Temperature-dependent material parameters are fitted based on experimental results from NIMS fatigue datasheets [7] and linearly interpolated in the LMM framework. The yield stress σ_y in EPP model is determined by 0.2% of plastic strain from the R-O model in Fig. 3a. The effect of cyclic hardening is considered in LMM using the R-O model as follows,

$$\frac{\Delta\varepsilon_t}{2} = \frac{\Delta\sigma_t}{2\bar{E}} + \left(\frac{\Delta\sigma_t}{2B}\right)^{\frac{1}{\beta}} \tag{1}$$

$$\bar{E} = \frac{3E}{2(1+\nu)} \tag{2}$$

where $\Delta\varepsilon_t$ is the total strain range; $\Delta\sigma_t$ is the total stress range; B and β are material parameters; $\bar{E}$ is the effective elastic modulus; E is the Young's modulus and ν is the Poisson's ratio. All the material parameters used are listed in Table 1.

TABLE 1 - Temperature dependent material properties

Temperature (ºC)	$\bar{E}$ (MPa)	ν	B (MPa)	β	σ_y (MPa)
20			784.181	0.113	389.432
300			635.862	0.096	350.069
400	182000	0.3	603.499	0.091	342.206
500			588.622	0.109	299.356
600			348.693	0.052	252.593

The creep constitutive relationship is implemented in LMM using the time-hardening power-law equation, as well as the Arrhenius law to consider non-isothermal effect. The creep strain data for 2.25Cr-1Mo in various temperature is obtained from

NIMS creep datasheets [8] where both primary and secondary stage of creep can be fitted using the proposed Norton-Bailey equation as follows,

$$\dot{\varepsilon}^c = A^* \sigma^n \Delta t^m \exp\left(-\frac{Q}{RT}\right) \tag{3}$$

where $\dot{\varepsilon}^c$ is the creep strain rate; σ is the applied stress; Δt is the creep dwell time; Q is the activation energy; R is the global gas constant; T is temperature in Kelvin; A^*, n, m are material parameters.

For damage evaluation, the low-cycle fatigue damage is assessed using the ε-N curve for 2.25Cr-1Mo at 500 ºC provided by [7]. The relationship between the number of cycles to failure N_f and the total strain range ε_t is fitted using a piecewise function which consists of 2 reverse power-law functions:

$$N_f = \begin{cases} D_1 \varepsilon_t^{-p_1}, & \varepsilon_t < 0.00494 \\ D_2 \varepsilon_t^{-p_2}, & \varepsilon_t \geq 0.00495 \end{cases} \tag{4}$$

$$\omega_f = 1/N_f \tag{5}$$

where N_f is the number of cycles to fatigue failure; ω_f is the fatigue damage per cycle; ε_t is the total strain range; D_1, D_2, p_1, p_2 are material parameters.

The creep damage is evaluated based on the creep rupture data for 2.25Cr-1Mo at 450 ºC provided by [8]. The curve is expressed by a reverse power-law relationship and fitted using the least squares method. In the LMM, the average stress $\bar{\sigma}$ during dwell is first calculated by numerically integrating the stress over the dwell time Δt. Then the number of cycles to failure N_c is determined as follows,

$$t^* = C\bar{\sigma}^{-k} \tag{6}$$

$$N_c = \frac{t^*}{\Delta t} \tag{7}$$

$$\omega_c = 1/N_c \tag{8}$$

where t^* is time to rupture; $\bar{\sigma}$ is the average stress; N_c is the number of cycles to creep failure; ω_c is the creep damage per cycle; Δt is the creep dwell time; C, k are material parameters.

In terms of creep-fatigue damage interaction, a bi-linear damage rule is adopted from ASME III-1 [9] as shown in Fig. 3b. The interception coordinate of 2 lines (c, f) for 2.25Cr-1Mo is $(0.1, 0.1)$. In this case, a point within the structure is considered to be creep-dominant if creep damage ω_c is greater than fatigue damage ω_f, or fatigue-dominant otherwise. The total number of cycles to failure N is evaluated as follows,

$$N = \begin{cases} \left(\omega_f + \frac{\omega_c(1-f)}{c}\right)^{-1}, & \omega_c < \omega_f \\ \left(\omega_c + \frac{\omega_f(1-c)}{f}\right)^{-1}, & \omega_c \geq \omega_f \end{cases} \tag{9}$$

where N is the number of cycles to failure; ω_f is fatigue damage per cycle; ω_c is creep damage per cycle; $c = 0.1$ and $f = 0.1$.

It is worth noting that both the fatigue and creep damage calculation processes use temperature-independent material parameters for ease in calculation. All the material parameters shown above are given in Table 2.

TABLE 2 - Material constants for 2.25Cr-1Mo

Creep strain rate	
A^* ($\mathrm{MPa^{-n} \cdot h^{-m}}$)	9.900E+06
n	6.020
m	-0.470
Q (kJ/mol)	368000
R (kJ/mol/K)	8.314
Fatigue damage	
D_1	0.126
D_2	1.415E-17
p_1	2.073
p_2	8.988
Creep damage	
C ($\mathrm{MPa^k \cdot h}$)	1.650E+34
k	11.899

RESULTS AND DISCUSSIONS

According to ASME Code Case 2605 [5], a ratcheting analysis is required to check whether the elastic shakedown state is achieved for all points in the structure. If not, a full inelastic analysis should be done instead of a simplified procedure for the creep-fatigue assessment purpose. Therefore, a shakedown analysis is first performed using the shakedown module in LMM framework, as shown in Fig. 4. The shakedown analysis considers temperature-dependent yield stress listed in Table 1 and the Elastic-Perfectly-Plastic (EPP) constitutive model. The temperature T is normalised by the reference temperature condition T_0, which is the normal operating temperature field given in Fig. 1. Also, the inner pressure P is normalised by the reference pressure $P_0 = 10$ MPa. The shakedown boundary provides a criterion for the judgement of structural response: for load cases inside the shakedown envelop, the structural

response is pure elastic or elastic shakedown; for load cases outside the shakedown envelop, the structure response is plastic shakedown or ratchetting. A total of 6 load cases are studied here with various inner pressure *P*, as shown in Fig. 4. It is worth to mention that the normal operating condition defined as load case (4) is slightly outside the shakedown boundary. The setup in LMM is also presented in Fig. 4, for which 5 load instances are set to simulate a full operating cycle. After a number of iterations, the LMM eventually produces the detailed steady-state information for every load instances which can be further post-processed for creep-fatigue life assessment.

To make the creep-fatigue assessment more precise and less conservative, the cyclic hardening effect of 2.25Cr-1Mo is considered using the temperature-dependent Ramberg-Osgood (R-O) inelastic model. The creep constitutive equation considers non-isothermal Norton-Bailey law and the operating condition is load case (4) in Fig. 4. The material constants for the R-O model are listed in Table 1. The influence of dwell time on the hysteresis loops for #335 is shown in Fig. 5. A total number of 6 different dwell time is considered for this case: 10, 100, 1000, 10000,100000, and 1000000 hours. Due to the consideration of cyclic hardening effect, a nonlinear segment can be seen during loading and unloading stage. The end of dwell stress-strain points in the hysteresis loops are connected using a spline curve to indicate a smooth evolution of stress-strain relationship during creep stage. With the increase of dwell time, the creep strain is gradually enlarged and causes greater creep ratchetting. Another important phenomenon called 'cyclically enhanced creep' can also be observed where the stress goes up to a higher value during the loading stage of next cycle, which creates a more considerable amount of creep strain for next cycle.

A series of tests with various loading conditions and dwell time have been conducted considering the temperature-dependent R-O model and the non-isothermal Norton-Bailey law. Damage assessment is performed with time fraction rule for creep damage evaluation using Eqs (6) ~ (8); total strain range calculation for fatigue damage evaluation using Eqs (4) and (5); bi-linear damage rule for creep-fatigue interaction damage evaluation using Eq. (9). As a result, over 30 case sets have been performed and shown in Table 3. Based on that, an analytic function has been fitted using the least squares method as follows,

$$N = \begin{cases} A_1 t^{-a_1} (0.1P)^{-b(t)}, & P < 10 \\ A_2 t^{-a_2} (0.1P)^{-c(t)}, & P \geq 10 \end{cases} \tag{10}$$

$$b(t) = b_1 \log t + b_2 \tag{11}$$

$$c(t) = c_1 \log t + c_2 \tag{12}$$

where *N* is the number of cycles to failure; *t* is the dwell time; *P* is the inner pressure; $A_1, a_1, A_2, a_2, b_1, b_2, c_1, c_2$ are parameters listed in Table 4. A comparison of the number of cycles to failure *N* obtained with the LMM and the analytic function has been made and presented in Fig. 6. It can be seen that all 30 data points can be placed snugly within a factor of 1.7 region, which proves the accuracy and reliability of the fitted analytic function.

TABLE 3 - Number of cycles to failure *N* for different load cases and dwell time

Load case	*P* (MPa)	Dwell time *t* (hours)				
		10	100	1000	10000	100000
1	2.5	23490	3912	684	197	102
2	5	7299	1417	263	83	50
3	7.5	2476	651	133	43	25
4	10	802	305	68	19	7
5	12.5	509	180	32	6	1
6	15	359	93	11	1	0

TABLE 4 - Parameters for the analytic function

A_1	a_1	A_2	a_2	b_1	b_2	c_1	c_2
4002.211	0.499	2880.050	0.521	-0.173	2.067	1.955	-0.649

CONCLUSIONS

A comprehensive creep-fatigue life assessment on a typical hydrogenation reactor made of 2.25Cr-1Mo steel has been performed by using the latest developed LMM framework. The design limit is determined by the shakedown analysis using the LMM shakedown module. A total of 6 load cases is then chosen based on the structural shakedown boundary with the inner pressure *P* ranging from 2.5 MPa to 15 MPa and a constant normal operating thermal condition. Five different creep dwell time is also considered ranging from 10 hours to 100000 hours. After that, a series of creep-fatigue analysis is conducted using the LMM eDSCA module. Finally, an analytic function is fitted based on the creep-fatigue interaction damage results for design purpose, and it is compared to the existing data points for verification. The temperature-dependent constitutive material models adopted include EPP model for shakedown analysis, R-O model for creep-fatigue damage assessment, and Norton-Bailey law for creep dwell computation. The damage evaluation process considers time fraction rule for creep damage evaluation, ε-N curve and total strain range for fatigue damage evaluation, and bi-linear damage rule for total damage evaluation. Several significant phenomena including ‘thermal ratchetting’, ‘cyclically enhanced creep’ and ‘creep enhanced

plasticity' are observed and appropriately discussed in this paper. The fitted analytic function has also been confirmed to be precise and conservative by allowing an error factor of 1.7. Therefore, it is of great feasibility to implement the LMM framework as part of the CC 2605 for improved design efficiency and reliability.

ACKNOWLEDGMENTS

The authors gratefully acknowledge the supports from the National Natural Science Foundation of China (51828501), Royal Society (IEC\NSFC\181071), University of Strathclyde and East China University of Science and Technology during the course of this work.

REFERENCE LIST

(1) X. Wu, Z. Zhao, X. Chen, *J. Mech. Eng* **51(6),** pp. 51–57 (2015).

(2) D. Barbera, *On the evaluation of high temperature creep-fatigue responses of structures*, University of Strathclyde, 2017.

(3) X.T. Zheng, Z.Y. Ma, H.F. Chen, J. Shen, *Key Eng. Mater*. **795,** pp. 383–388 (2019).

(4) A. Boiler, *P.V. Code, Section VIII, Division 2: Alternative rules, rules for construction of pressure vessels*, American Society of Mechanical Engineers, New York, 2007.

(5) A. Boiler, *Cases of ASME boiler and pressure vessel code, Case 2605*, American Society of Mechanical Engineers, New York, 2017.

(6) D. Barbera, H. Chen, Y. Liu, F. Xuan, *J PRESS VESS-T ASME*, **139(5),** pp. 051101 (2017).

(7) *Data sheets on long-term, high temperature low-cycle fatigue properties of SCMV 4 (2.25Cr-1Mo) steel plate for boilers and pressure vessels*, NIMS creep data sheet no. 94. Tsukuba, Japan: National Institute for Materials Science, 2004.

(8) *Data sheets on the elevated-temperature properties of quenched and tempered 2.25Cr-1Mo steel plates for pressure vessels (ASTM A542/A542M)*, NIMS creep data sheet no. 36B. Tsukuba, Japan: National Institute for Materials Science, 2003.

(9) A. Boiler, *P.V. Code, Section III Division 1: Rules for Construction of Nuclear Facility Components*, American Society of Mechanical Engineers, New York, 2015.

(10) R. Ainsworth, *R5: Assessment procedure for the high temperature response of structures*, British Energy Generation Ltd 3, 2003.

FIGURES

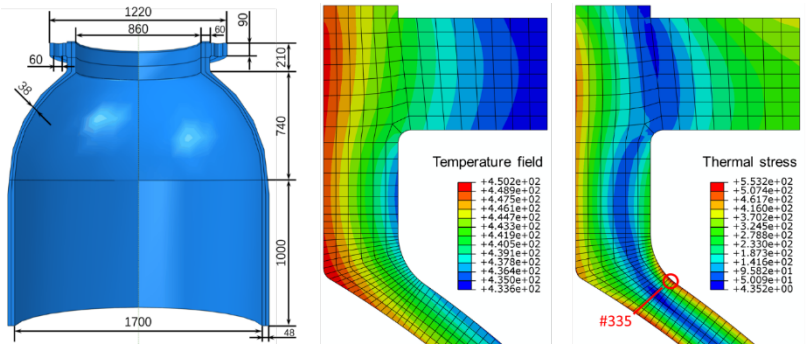

FIGURE: 1 - Geometry and thermal analysis of the hydrogenation reactor.

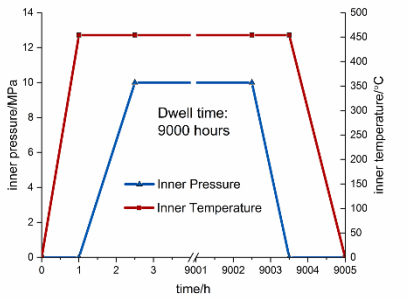

FIGURE: 2 - Industrial loading history for a normal operation cycle.

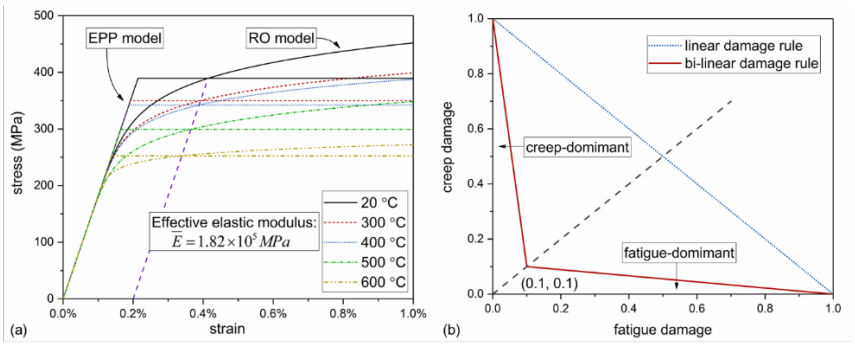

FIGURE: 3 - Material properties of 2.25Cr-1Mo: (a) temperature dependent inelastic constitutive models; (b) creep-fatigue damage interaction diagram.

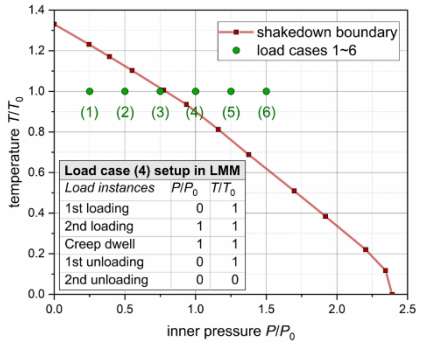

FIGURE: 4 - Shakedown boundary of the structure and chosen load cases for creep-fatigue analysis.

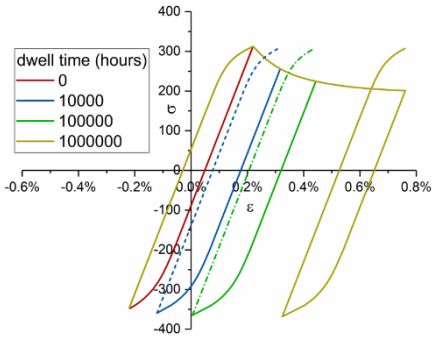

FIGURE: 5 - Hysteresis loops for #335 using the Ramberg-Osgood (R-O) model with application of load case (4) and various dwell time.

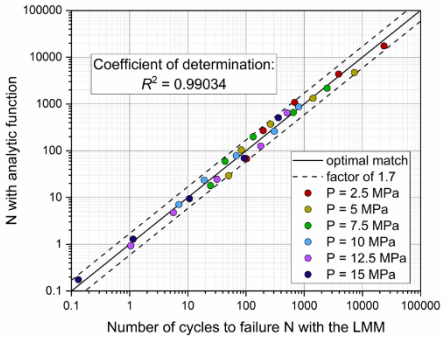

FIGURE: 6 - Comparison of the number of cycles to failure N for different pressure levels obtained with the LMM and the analytic function.